Boosting Oxygen Evolution Reaction Performance via Hydrothermally Synthesized 4A Zeolite-Supported Ni Catalysts: Structure–Activity Relationship Investigation

Xiuzhen Xie[a,b,*], Chenglu Hu[a,c], Cao Luo[a], QiuJie Shi[a], Yongyang Wang [a], Zhuohan Xie [a], Zihan Yao [a], Qizhi Le[a], Wen-yi Hu,[a*]

[a]*College of Chemistry and Material Science, Longyan University, Longyan 364012, Fujian Province, People's Republic of China; Fujian Provincial Colleges;*

[b]*Department of Materials Science and Engineering, College of Materials, Xiamen University, No. 422 Siming South Road, Xiamen, 361005, Fujian Province, China;*

[c]*Key Lab of Electromagnetic Processing of Materials, Ministry of Education, Northeastern University, Shenyang, China，People's Republic of China;*

*Corresponding authors. E-mail: huwenyi@lyun.edu.cn

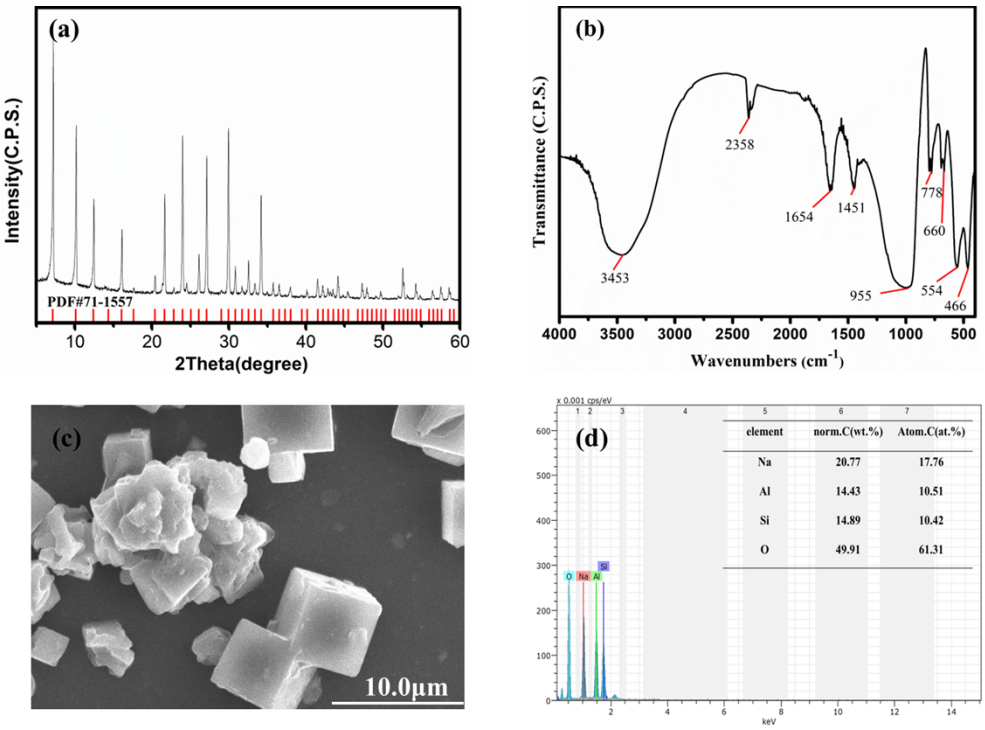

Figure S1 Powder X-ray diffraction (PXRD) pattern, Fourier transform infrared (FT-IR) spectrum, scanning electron microscopy (SEM) image, and energy-dispersive X-

ray spectroscopy (EDS) spectrum of the pristine 4A zeolite.

Table S1 Inductively coupled plasma (ICP) spectroscopy test results of all samples (4A, 4AP, and 4A/xNi composites with x = 20, 40, 60, 80 wt.%), including the elemental composition and corresponding concentration data.

Samples	Ni (mg/L)	Al (mg/L)
4A	0.238	157.280
4AP	0.231	142.760
4A/20wt.% Ni	38.409	139.945
4A/40wt.% Ni	72.597	123.269
4A/60wt.% Ni	109.169	158.927
4A/80wt.% Ni	116.667	163.277

*The most sensitive and least interfered analytical line: Ni 231.604; Al 396.153.

*Each sample is tested three times, Error range: ±0.001 mg/L.

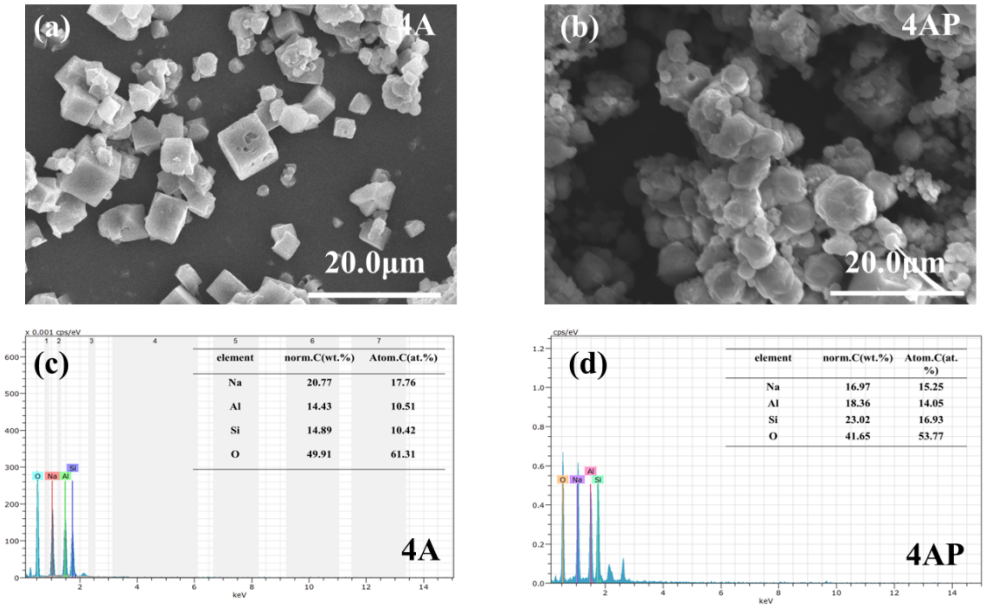

Figure S2 Scanning electron microscopy (SEM) images and energy-dispersive X-ray spectroscopy (EDS) spectra/mappings of pristine 4A zeolite and 4AP composite

material.

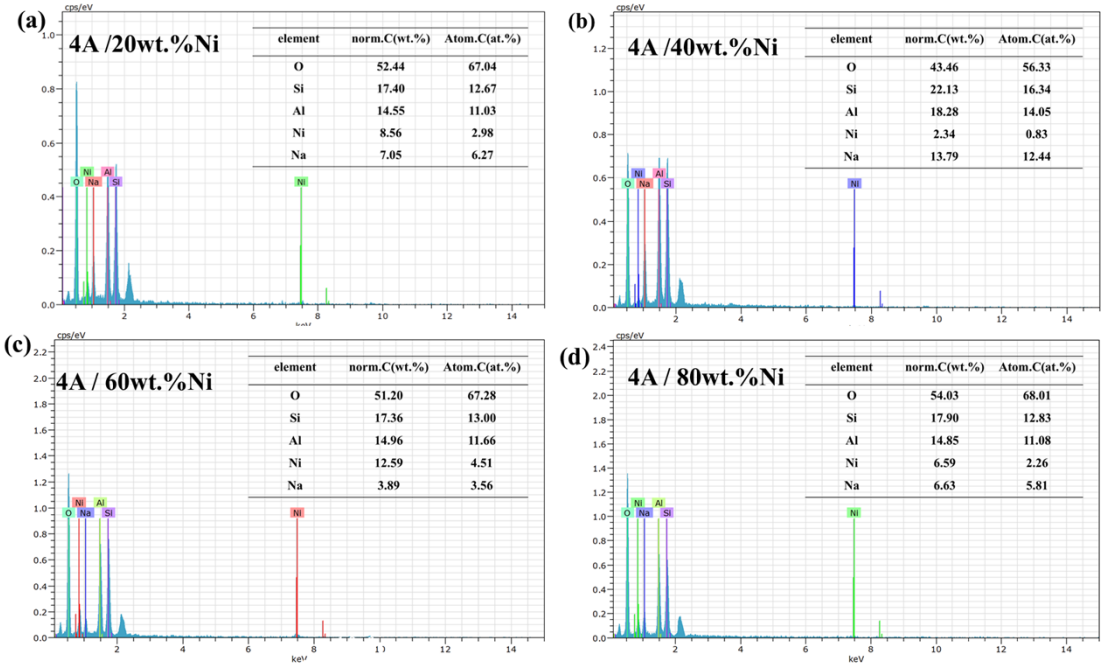

Figure S3 Energy-dispersive X-ray spectroscopy (EDS) spectra/elemental mappings of 4A/xNi composite materials with x = 20, 40, 60, 80 wt.%.

Table S2 Specific surface area data of Ni-ion loaded 4A zeolite composites (4A/xNi with x = 20, 40, 60, 80 wt.%), determined via Brunauer-Emmett-Teller (BET) surface area analysis.

Samples	**Specific Surface Area** m^2/g
4A	1.54
4AP	2.52
4A/20wt.% Ni	6.72
4A/40wt.% Ni	13.13
4A/60wt.% Ni	45.23
4A/80wt.% Ni	46.63

Table S3 Turnover frequency (TOF) values of all tested samples (4A, 4AP, and 4A/xNi composite materials with x = 20, 40, 60, 80 wt.%), calculated based on the

catalytic performance test results under specific reaction conditions.

Samples	I(mA/cm^2)	Q(mA*S)	Z	Z_2	TOF(S^{-1})
4A/20wt.%Ni	7.4	7	4	1	0.26
4A/40wt.%Ni	5.1	16	4	1	0.08
4A/60wt.%Ni	8.3	12	4	1	0.17
4A/80wt.%Ni	17.6	12	4	1	0.37

Z represents the electron transfer number (in the OER reaction, Z = 4)

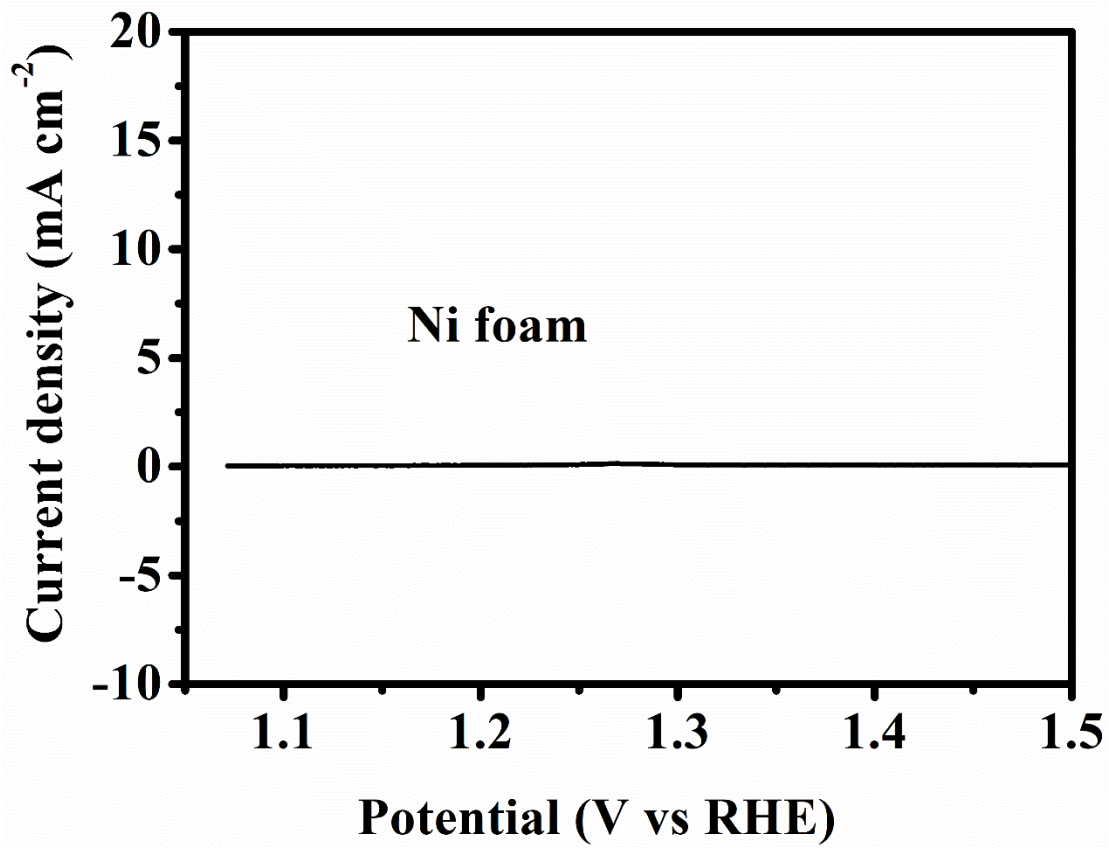

Figure S4 Linear sweep voltammetry (LSV) curve of the nickel (Ni) foam reference electrode, tested under the same electrochemical measurement conditions as the target samples (4A, 4AP, and 4A/xNi composites).

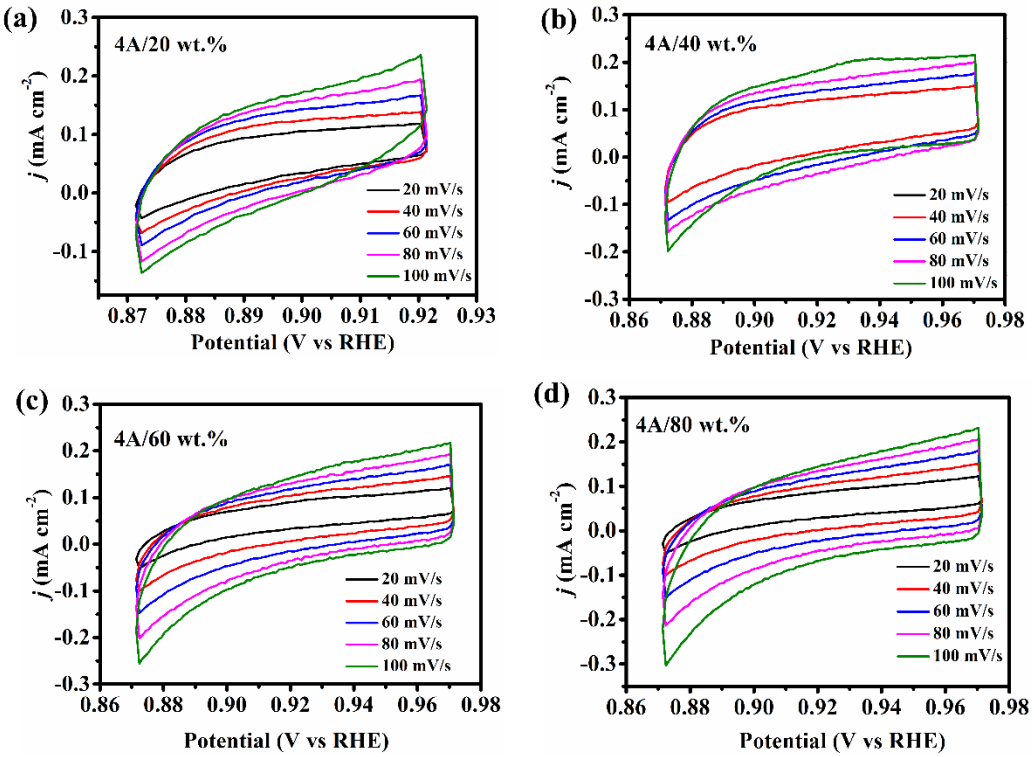

Figure S5 Cyclic voltammetry (CV) curves of all tested samples (4A, 4AP, and 4A/xNi composite materials with x = 20, 40, 60, 80 wt.%), recorded under the same electrochemical measurement conditions to evaluate their redox behavior and electrochemical activity.

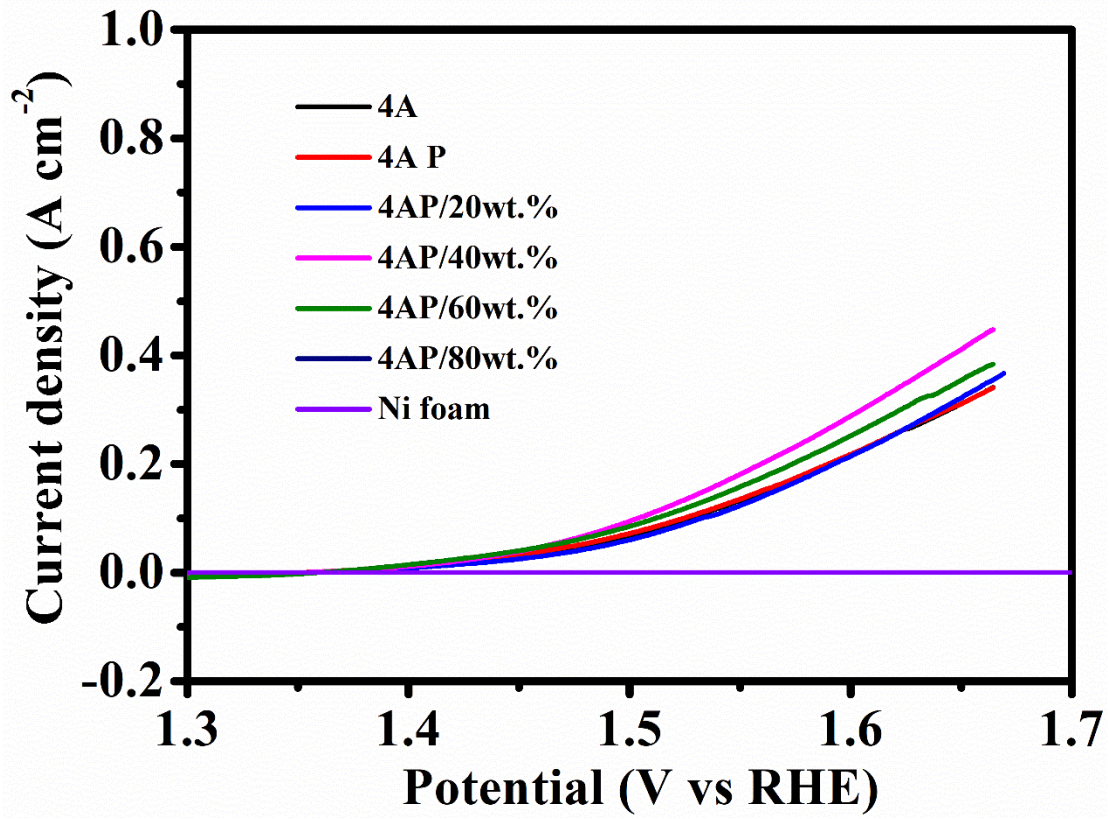

Figure S6 Linear sweep voltammetry (LSV) curves of all tested samples, including 4A zeolite, 4AP, and 4A/xNi composite materials with varying Ni loadings (x = 20, 40, 60, 80 wt.%), recorded under consistent electrochemical measurement conditions (e.g., electrolyte, scan rate, potential range) to evaluate their electrocatalytic activity for the target reaction.

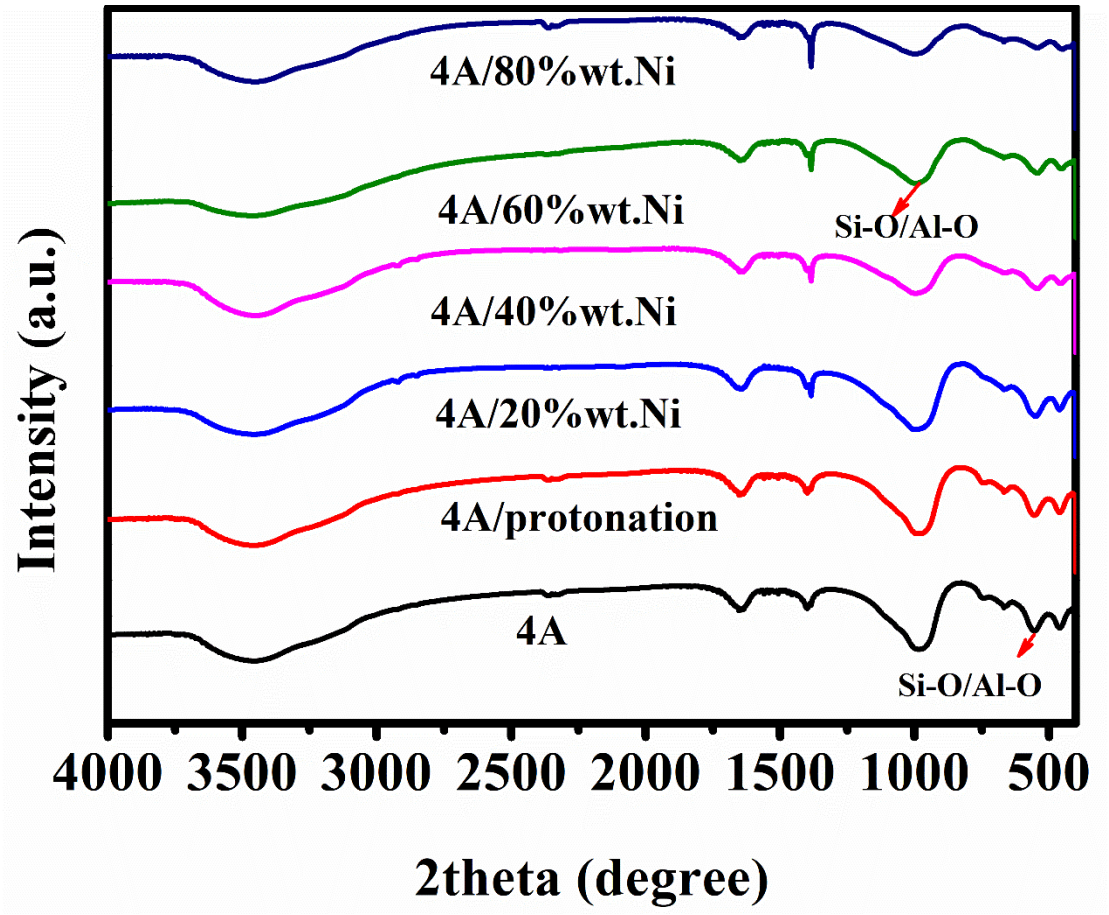

Figure S7 Fourier transform infrared (FTIR) spectra of all tested samples, including pristine 4A zeolite, 4AP, and 4A/xNi composite materials with varying Ni loadings (x = 20, 40, 60, 80 wt.%), recorded to characterize the functional groups, chemical bonds, and structural changes of the materials.

The sample exhibited characteristic absorption peaks of 4A zeolite at 990, 660, 554, and 466 cm^{-1}. Among them, the peak at 995 cm^{-1} corresponds to the antisymmetric stretching vibration of the T-O bond; the shoulder peak in the 1000 - 1200 cm^{-1} range was the antisymmetric stretching vibration of the T-O-T bond; the peak at 660 cm^{-1} was the symmetric stretching vibration of the T-O bond; the peak at 554 cm^{-1} was the extension vibration of the double hexagonal ring; the peak at 466 cm^{-1} was the bending vibration of the T-O bond. The peak at 1654 cm^{-1} corresponded to the bending vibration of -OH, and the peak at 3424 cm^{-1} corresponded to the absorption peak of the bound water in 4A zeolite.

Table S4 Quantitative correlation diagram of activity with ECSA, pore volume and Ni content

Samples	Ni (wt.%)	C_{dl} (μF cm^{-2})	ECSA (cm^2)	Pore Volume (cm^3/g)	Ones et (V)	**TOF (s^{-1})**
4A/20wt.%Ni	20	16.0	0.40	0.001	1.406	0.26
4A/40wt.%Ni	40	18.9	0.47	0.002	1.396	0.08
4A/60wt.%Ni	60	98.3	2.46	0.004	1.389	0.17
4A/80wt.%Ni	80	12.6	0.32	0.005	1.422	0.37